Title
Modified release from lipid bilayer coated mesoporous silica nanoparticles using PEO-PPO-PEO triblock copolymers

Authors
Rahman, M
Yu, E
Forman, E
et al.

Publication Date
2014-09-04

DOI
10.1016/j.colsurfb.2014.08.013

Peer reviewed

Colloids and Surfaces B: Biointerfaces 122 (2014) 818–822

Contents lists available at ScienceDirect

Colloids and Surfaces B: Biointerfaces

journal homepage: www.elsevier.com/locate/colsurfb

Modified release from lipid bilayer coated mesoporous silica nanoparticles using PEO–PPO–PEO triblock copolymers

Masoud Rahman[a], Erick Yu[a], Evan Forman[a], Cameron Roberson-Mailloux[a], Jonathan Tung[a], Joseph Tringe[b], Pieter Stroeve[a,*]

[a] Department of Chemical Engineering and Materials Science, University of California Davis, Davis, CA 95616, USA
[b] Lawrence Livermore National Laboratory, Livermore, CA 94550, USA

ARTICLE INFO

Article history:
Received 2 June 2014
Received in revised form 5 August 2014
Accepted 12 August 2014
Available online 20 August 2014

Keywords:
Drug delivery
Controlled release
Diffusion
Critical micelle concentration
Pluronic

ABSTRACT

Triblock copolymers comprised of poly(ethylene oxide)–poly(propylene oxide)–poly(ethylene oxide) (PEO–PPO–PEO, or trade name Pluronic) interact with lipid bilayers to increase their permeability. Here we demonstrate a novel application of Pluronic L61 and L64 as modification agents in tailoring the release rate of a molecular indicator species from 1,2-dioleoyl-sn-glycero-3-phosphocholine (DOPC) bilayer-coated superparamagnetic Fe_3O_4/mesoporous silica core–shell nanoparticles. We show there is a direct relationship between the Pluronics' concentration and the indicator molecule release, suggesting Pluronics may be useful for the controlled release of drugs from lipid bilayer-coated carriers.

1. Introduction

Mesoporous silica is a versatile and useful template for biomedical and catalytic support applications. The commonly synthesized template of mesoporous silica nanoparticles, MCM-41, is composed of well-ordered arrays of hexagonally close-packed cylindrical nanopores, where the pores are approximately 3–4 nm diameter [1]. Because of the high porosity and large effective surface area of MCM-41 nanoparticles, they have been used effectively for loading a wide range of molecules, including anticancer drugs such as doxorubicin (DOX) [2], markers including green fluorescent protein (GFP) [3], and gene therapy agents such as small interfering RNA (siRNA) [4]. By having drugs encapsulated inside the pores of mesoporous silica, advanced target and release mechanisms can be implemented, such as those triggered by changes in temperature [5], pH [6], specific target binding [7], or the presence of a particular solute [8]. Triggered release is critical for targeted delivery of toxic or insoluble drugs. In our previous work [9] we showed that by lipid bilayer encapsulation of superparamagnetic iron oxide nanoparticles (SPIONs) inside mesoporous silica, a magnetically responsive, core–shell drug carrier can be synthesized. SPIONs have been extensively used in drug delivery and for treating localized hyperthermia [10]. Their integration with mesoporous silica results in a combination of high surface area and magnetic response in a single particle. In this study, the presence of SPIONs inside mesoporous silica was helpful in magnetic separation and removal from solution.

Release studies done in our previous work suggested that a modification was needed to design a faster response toward a trigger stimulus. Simulation and experimental studies done by others have provided insight into Pluronic–lipid interactions and their incorporation into lipid bilayers. Pluronics were shown to enhance membrane fluidity [11] and possibly to create channels or pores in the bilayer [12,13]. Due to the diversity of Pluronic triblock copolymers, functional behavior differs depending on the copolymerization ratio and total molecular weight of the polymer chain. It has been shown that Pluronics with smaller molecular weight and less hydrophilic contribution resulted in a greater lipid membrane permeability [14]. By this rationale, Pluronic L61 was selected for use with our lipid coated Fe_3O_4/mesoporous silica nanoparticles due to its high degree of interaction with the lipid membrane. Fig. 1 shows possible conformations of Pluronic L61 as it interacts with a lipid bilayer based on previously reported computational studies [14]. By local distortion in the lipid membrane, drug cargo contents can be diffused across the bilayer with greater ease. Methylene blue (MB) was employed as an indicator of drug release from superparamagnetic/mesoporous silica–lipid–Pluronic (SMLP) nanoparticles. A similar triblock copolymer, Pluronic L64, was used

* Corresponding author. Tel.: +1 5303049748
E-mail address: pstroeve@ucdavis.edu (P. Stroeve).

http://dx.doi.org/10.1016/j.colsurfb.2014.08.013
0927-7765/

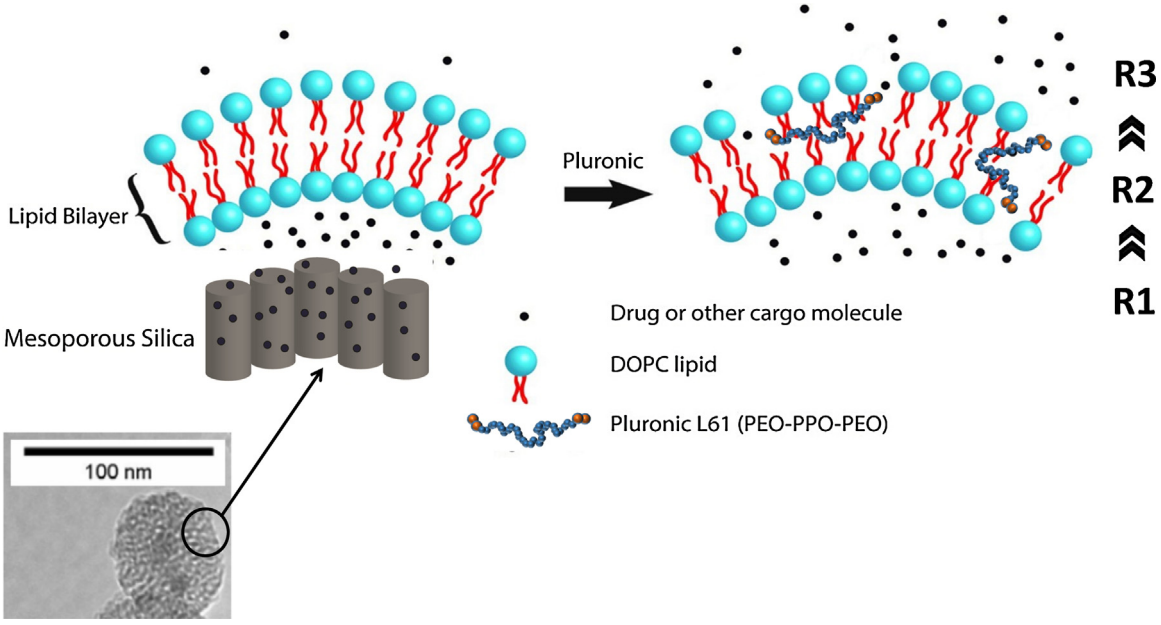

Fig. 1. Schematic showing of the intercalation of Pluronic L61 with a segment of lipid bilayer. For the Pluronic, the red PEO blocks are hydrophilic and the dark blue PPO blocks are hydrophobic. R1, R2, and R3 represent different mass transfer resistances (for the cargo molecules) for inside the nanoparticle, the lipid bilayer, and the solution. (For interpretation of the color information in this figure legend, the reader is referred to the web version of the article.)

as a comparison to Pluronic L61 to better understand the role of the hydrophobic structure of Pluronics in the interaction with the lipid bilayer. Both Pluronics share identical PPO content, but due to the fourfold PEO content and thus greater hydrophilicity in L64, its ability to perturb the bilayer is expected to be less than L61.

2. Materials and methods

Superparamagnetic iron oxide, Fe_3O_4, was synthesized by a standard co-precipitation method [15] and further coated with a mesoporous silica shell using the Stöber process [16]. The experimental synthesis of core–shell nanoparticles and lipid coating was adapted from our previous work [9]. Pluronics L61 and L64 were provided by BASF and have molecular weights of approximately 2000 g/mole and 2900 g/mole with PEO wt% of approximately 10 and 40% respectively. The DOPC lipid was obtained from Sigma Aldrich. The final solution comprised of SMLP nanoparticles contained about 2.82 mg/mL of nanoparticles in 2.48 mg/mL of DOPC.

The size and morphology of the synthesized core–shell nanoparticles were investigated by transmission electron microscopy (TEM) on a Philips CM12 at 100 keV. Dynamic light scattering (DLS) was used to determine the particle size distribution; measurements were performed with a Malvern Nano S90. The as-synthesized core–shell nanoparticles had some aggregation. The larger agglomerates were suspected to have incomplete lipid coating and potentially complicated the release process compared to the spherical release of a single core–shell nanoparticle. To decrease the particle size polydispersity the as-synthesized nanoparticles were re-dispersed in DI water, placed in an ultrasonic bath for 10 min to break the agglomerates, and followed by 5 min of centrifugal separation (2000 rpm) of the supernatant.

Due to the lack of room temperature (24.5 °C) CMC values for Pluronic L61 in the literature, surface tensiometer measurements were done for both L61 and L64. A small glass petri dish filled with 10 mL of DI water (18 MΩ) was used with a NIMA PS4 pressure sensor. Small increments of 2–200 μL Pluronic L61 or L64 prepared at varying concentrations were added with a glass syringe to the petri dish. Measurements were collected once surface tension readings stabilized.

UV–visible spectrometry measurements were performed with a Varian Cary UV-Vis 300 to record absorbance of MB. The release tests with Pluronic L61 or L64 were done over a period of 2 h at room temperature (RT, 24.5 °C). Prior to addition of Pluronic, the nanoparticle solutions were evenly dispersed into plastic vials, each containing 6 mL. To measure initial $t = 0$ release, 1 mL samples were taken out. The required concentration of Pluronic was immediately added to the remaining 5 mL left on the shaker. At each interval time 1 mL of solution was collected and the nanoparticles were removed by magnetic separation and the supernatant was used for UV–vis measurements. The presence of nanoparticles inside the sample caused a scattering issue, which affected the UV–vis measurements. Normalized cumulative release values were determined by the release amount as a fraction of the maximum capacity determined by addition of sodium dodecyl sulfate (SDS) to completely remove the lipid bilayer.

3. Results

The mesoporous structure of silica shell and the presence of SPIONs inside the silica shell can be seen in the representative TEM images in Fig. 2. These and other similar images revealed that typical core–shell nanoparticle contain multiple SPIONs, each with SPION being ~20 nm diameter.

The average particle size distribution process was characterized by dynamic light scattering (DLS). The separation process was verified by the DLS data in Fig. 3 to be effective in removing the original bimodal distribution. The bimodal distribution of nanoparticles shows polydispersity, while the centrifugal segregation resulted in a monodisperse distribution with the average size of around 128 nm, consistent with TEM images such Fig. 2.

To investigate the role of Pluronic concentration on release rate concentrations were chosen based on the critical micelle concentration (CMC). Pluronic concentrations were kept below the CMC value to ensure unimer conformation and to prevent any micelle formation (Table 1). The CMC values commonly reported for L61 and L64 are at physiological temperature (PT, 37 °C) but, as Alexandridis and Hatton [17] had demonstrated, there is a strong

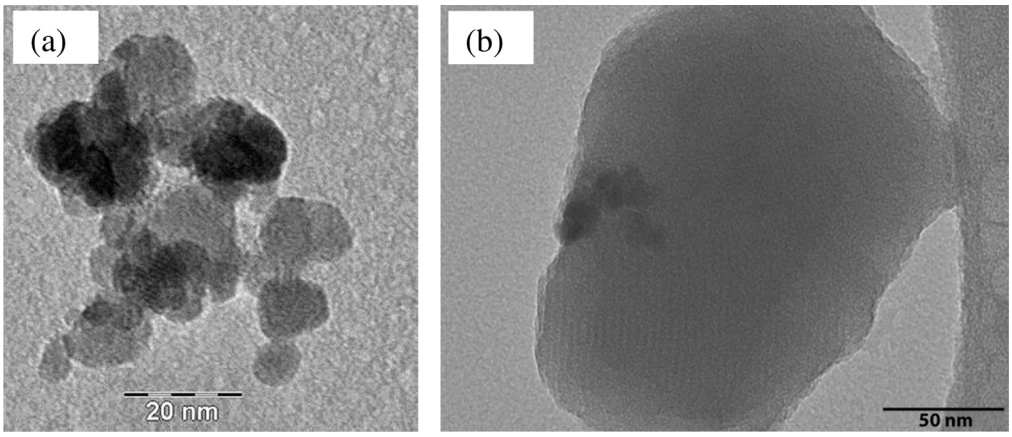

Fig. 2. TEM images of (a) the SPIONs (Fe_3O_4), (b) SPION/mesoporous silica core shell nanoparticles.

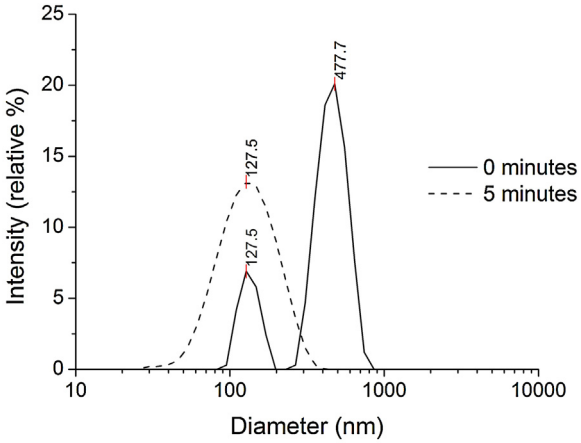

Fig. 3. Size distribution of core–shell nanoparticles before and after 5 min of centrifuge.

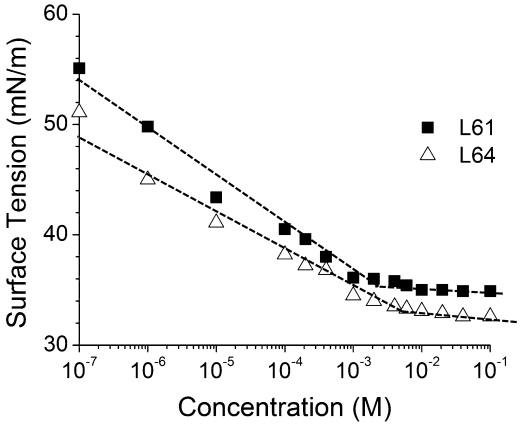

Fig. 4. Surface tension as a function of Pluronic concentration at RT. The CMC values were calculated by intersection of the linear extrapolation and the asymptote regime.

temperature–CMC relationship that can cause orders of magnitude differences for the CMC value.

Therefore, we measured the CMC at room temperature (RT) using a NIMA PS4 surface pressure sensor by the Wilhelmy plate method. From surface tensiometer results in Fig. 4, the CMC values for L61 and L64 at RT are found to be 1.55×10^{-3} M and 4.28×10^{-3} M, respectively. These values at RT are higher within an order of magnitude compared to values of 1.1×10^{-4} M and 4.8×10^{-4} M at 37 °C [18]. Previous surface tensions for L64 [19] reported at 25 °C show very close agreement with our results at RT.

The effect of L61 and L64 and their concentration on release were studied to understand the effect of Pluronic structure and concentration. Table 1 summarizes the sample names and their conditions. The release measurements from SMLP nanoparticles in Fig. 5(a) indicate that the MB release increases with increasing the Pluronic concentration. Fig. 5(b) shows the MB release from SMLP nanoparticles after 60 min for varying Pluronic L61 concentration at RT and PT.

Table 1
Type and concentration of Pluronic in each sample and Pluronic percentage CMC at physiological (PT) and room temperature (RT).

Sample	Pluronic concentration (M)	Percentage of Pluronic CMC (PT)	Percentage of Pluronic CMC (RT)
C0	0	0	0
L61-C1	1.10E−05	10%	0.71%
L61-C2	3.30E−05	30%	2.13%
L61-C3	5.50E−05	50%	3.55%
L64-C1	4.80E−05	10%	1.12%
L64-C2	1.44E−04	30%	3.36%
L64-C3	2.40E−04	50%	5.61%

Different parameters such as molecular weight, PPO/PEO composition ratio, and PPO block length can affect the properties of Pluronics [17]. To evaluate the role of ethylene oxide (PEO) on the interaction of Pluronic with lipid bilayer and the release rate, two Pluronics with the same PPO length and very close molecular weight, L61 and L64 are compared. L64 has 40 wt% PEO and L61 contains 10 wt% which makes L64 more hydrophilic. Fig. 6 shows the cumulative release of SMLP nanoparticles as a function of time for Pluronic L61 and L64 at RT and as a function of concentration for various release times.

4. Discussion

The experiment results show the critical role played by the lipid bilayer in controlling the rate of MB release from the SMLP nanoparticles. Initially, a simplified error function based fitting was attempted with the cumulative release data from Fig. 5(a). This would match simplified Fick's diffusion. However, due to poor fitting, a logarithmic equation was used instead here.

$$y = \frac{C_t}{C_{max}} = a - b\ \ln(t) \quad (1)$$

where a and b are constants, y shows the cumulative release percentage, C_{max} represents the maximum loading capacity as determined from addition of sodium dodecyl sulfate (SDS) to

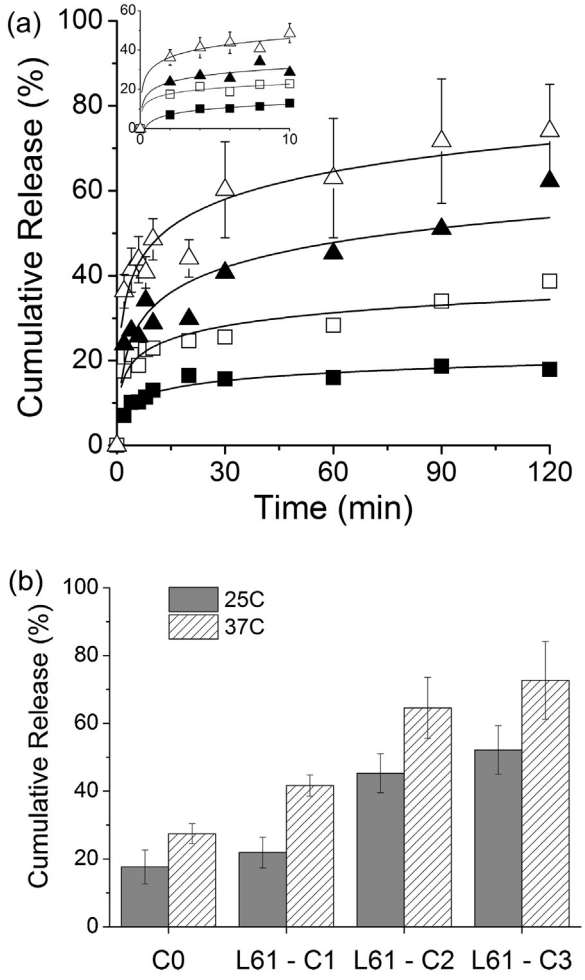

Fig. 5. (a) Cumulative release of MB from SMLP nanoparticles over time for various Pluronic L61 concentrations at RT. The solid curves show the fitting. Error bars are only shown for sample L61-C3 in order to maintain the figure clarity. However, the experiments were carried out with $n = 5$ and the standard deviation (SD) being ±0.77% (times less than 10 min) to 18% (for times more then 30 min). The SD increased at longer times. The inset shows the first 10 min of the release. The MB release measurements from SMLP nanoparticles after 60 min for varying Pluronic L61 concentration at RT and PT (b).

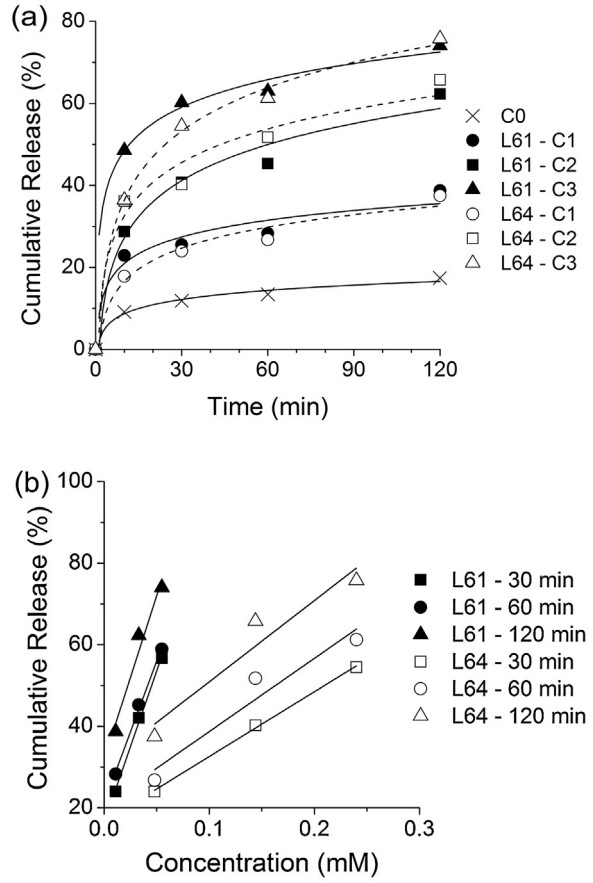

Fig. 6. The cumulative release of SMLP nanoparticles (a) as a function of time for Pluronic L61 and L64 at RT and (b) as a function of concentration for various release times. The solid lines are for the L61 data and the dashed lines are for the L64 data. The experimental error bars are not shown to maintain figure clarity, but for the L64 experiments, $n = 3$, the SD were ±0.51% (times less than 10 min) to 8.85% (times greater than 30 min). The number of experiments and SD for L61 is the same as Fig. 5.

remove the lipid bilayer completely, and C_t show the methylene blue concentration at time t.

The cumulative release of MB from SMLP nanoparticles is shown in Fig. 5(a). To determine the maximum dye loading, SDS was added to the control sample and upon addition, the solution showed immediate signs of methylene blue release (in less than 1 min). From this observation, and the fact that SDS is responsible for dissolving the lipid bilayer coating, diffusion of dye through the lipid bilayer is the rate determining step. The increase of MB release with Pluronic concentration indicates the effectiveness of Pluronic in decreasing the mass transport resistance in the lipid bilayer, and hence increasing the MB permeability of the lipid bilayer.

A previous report [17] showed that an increase of 10 °C in temperature can change the CMC by one order of magnitude. Therefore, the role of temperature on Pluronic L61–lipid interaction and release behavior was investigated at room temperature and physiological temperature (PT). According to Fig. 5(b), the release at PT has the same behavior as at RT. The increase in the release at higher temperature can be described based on a greater diffusion rate at greater temperatures, as well as greater fluidity and greater MB permeability of the lipid bilayer.

From the release behavior shown in Fig. 6(a), it can be seen that the difference between L61 and L64, as plotted, is marginal. This indicates that L61 and L64 have the same behavior when their concentrations are calculated as percentage of their CMCs. Since the CMC concentration of L61 is much lower than L64, at a particular percent-CMC concentration of L64, there is substantially less L61 present. By viewing the results as a function of the concentration in Fig. 6(b), it can be concluded that at a fixed concentration L61 is more effective than L64 in releasing the MB. The parallel slope lines indicate that the release rate is independent of time. The average slope for L61 was found to be 7.47% per mM, while for L64 it is 1.79% per mM. Interestingly, the fourfold difference between the two roughly correlates to the fourfold difference in PEO content between L61 and L64.

A similar conclusion was made by Batrakova et al. [20] when comparing the efficacy difference between P85 and L81. A greater distortion effect was seen with P85 at a fixed concentration due to its greater CMC value and thus, greater unimer concentration present at the CMC cut-off. When compared per unimer basis, our results agree with prior simulation results from Nawaz et al. [14] that L61 should cause greater lipid bilayer distortion compared to L64.

5. Conclusions

We have demonstrated that the release rate of lipid bilayer-coated core–shell nanoparticles can be finely tuned by Pluronics, a result which may aid the development of drug delivery systems.

Both Pluronic L61 and L64 showed a linear increase in release with respect to concentration. In particular, Pluronic L61 resulted in a four-fold greater release over L64, which can be associated to their PEO content, where the lower hydrophilicity causes greater distortion in the lipid membrane. Both Pluronics showed similar behavior at the same CMC-percentage concentration. It was shown that with a concentration of 5.61% CMC (at RT), nearly 75% of the loaded MB was released after 2 h. A similar result was achieved at physiological temperature, 37 °C, in 1 h, indicating that the elevated temperature increases diffusion of MB from the nanoparticles as expected. For physiological applications it is necessary to understand the long-term stability of Pluronic inside the lipid bilayer. Nevertheless, the application of Pluronic to lipid bilayers is promising for decreasing the required magnetic field and exposure times for triggered drug release.

Acknowledgements

This work was supported by the University of California Lab Fee Program through the Office of the President in Oakland, California. Parts of this work were performed under the auspices of the U. S. Department of Energy by Lawrence Livermore National Laboratory under Contract DE-AC52-07NA27344.

References

[1] J.S. Beck, J.C. Vartuli, W.J. Roth, M.E. Leonowicz, C.T. Kresge, K.D. Schmitt, C.T.W. Chu, D.H. Olson, E.W. Sheppard, A new family of mesoporous molecular sieves prepared with liquid crystal templates, J. Am. Chem. Soc. 114 (1992) 10834–10843.
[2] H. Meng, M. Liong, T. Xia, Z. Li, Z. Ji, J.I. Zink, A.E. Nel, Engineered design of mesoporous silica nanoparticles to deliver doxorubicin and P-glycoprotein siRNA to overcome drug resistance in a cancer cell line, ACS Nano 4 (2010) 4539–4550.
[3] I.I. Slowing, B.G. Trewyn, S. Giri, V.S.Y. Lin, Mesoporous silica nanoparticles for drug delivery and biosensing applications, Adv. Funct. Mater. 17 (2007) 1225–1236.
[4] C.E. Ashley, E.C. Carnes, K.E. Epler, D.P. Padilla, G.K. Phillips, R.E. Castillo, D.C. Wilkinson, B.S. Wilkinson, C.A. Burgard, R.M. Kalinich, J.L. Townson, B. Chackerian, C.L. Willman, D.S. Peabody, W. Wharton, C.J. Brinker, Delivery of small interfering RNA by peptide-targeted mesoporous silica nanoparticle-supported lipid bilayers, ACS Nano 6 (2012) 2174–2188.
[5] C. Liu, J. Guo, W. Yang, J. Hu, C. Wang, S. Fu, Magnetic mesoporous silica microspheres with thermo-sensitive polymer shell for controlled drug release, J. Mater. Chem. 19 (2009) 4764–4770.
[6] Q. Yang, S. Wang, P. Fan, L. Wang, Y. Di, K. Lin, F.-S. Xiao, pH-responsive carrier system based on carboxylic acid modified mesoporous silica and polyelectrolyte for drug delivery, Chem. Mater. 17 (2005) 5999–6003.
[7] D.P. Ferris, J. Lu, C. Gothard, R. Yanes, C.R. Thomas, J.-C. Olsen, J.F. Stoddart, F. Tamanoi, J.I. Zink, Synthesis of biomolecule-modified mesoporous silica nanoparticles for targeted hydrophobic drug delivery to cancer cells, Small 7 (2011) 1816–1826.
[8] E. Aznar, R. Villalonga, C. Gimenez, F. Sancenon, M.D. Marcos, R. Martinez-Manez, P. Diez, J.M. Pingarron, P. Amoros, Glucose-triggered release using enzyme-gated mesoporous silica nanoparticles, Chem. Commun. 49 (2013) 6391–6393.
[9] E. Bringas, O. Koysuren, D.V. Quach, M. Mahmoudi, E. Aznar, J.D. Roehling, M.D. Marcos, R. Martinez-Manez, P. Stroeve, Triggered release in lipid bilayer-capped mesoporous silica nanoparticles containing SPION using an alternating magnetic field, Chem. Commun. 48 (2012) 5647–5649.
[10] C.S.S.R. Kumar, F. Mohammad, Magnetic nanomaterials for hyperthermia-based therapy and controlled drug delivery, Adv. Drug Deliv. Rev. 63 (2011) 789–808.
[11] E. Batrakova, S. Lee, S. Li, A. Venne, V. Alakhov, A. Kabanov, Fundamental relationships between the composition of Pluronic block copolymers and their hypersensitization effect in MDR cancer cells, Pharm. Res. 16 (1999) 1373–1379.
[12] O.O. Krylova, P. Pohl, Ionophoric activity of Pluronic block copolymers, Biochemistry 43 (2004) 3696–3703.
[13] M. Schulz, A. Olubummo, W.H. Binder, Beyond the lipid-bilayer: interaction of polymers and nanoparticles with membranes, Soft Matter 8 (2012) 4849–4864.
[14] S. Nawaz, M. Redhead, G. Mantovani, C. Alexander, C. Bosquillon, P. Carbone, Interactions of PEO–PPO–PEO block copolymers with lipid membranes: a computational and experimental study linking membrane lysis with polymer structure, Soft Matter 8 (2012) 6744–6754.
[15] S. Laurent, D. Forge, M. Port, A. Roch, C. Robic, L. Vander Elst, R.N. Muller, Magnetic iron oxide nanoparticles: synthesis, stabilization, vectorization, physicochemical characterizations, and biological applications, Chem. Rev. 108 (2008) 2064–2110.
[16] W. Stöber, A. Fink, E. Bohn, Controlled growth of monodisperse silica spheres in the micron size range, J. Colloid Interface Sci. 26 (1968) 62–69.
[17] P. Alexandridis, T. Alan Hatton, Poly(ethylene oxide)–poly(propylene oxide)–poly(ethylene oxide) block copolymer surfactants in aqueous solutions and at interfaces: thermodynamics, structure, dynamics, and modeling, Colloid Surf. A: Physicochem. Eng. Aspects 96 (1995) 1–46.
[18] M.Y. Kozlov, N.S. Melik-Nubarov, E.V. Batrakova, A.V. Kabanov, Relationship between Pluronic block copolymer structure, critical micellization concentration and partitioning coefficients of low molecular mass solutes, Macromolecules 33 (2000) 3305–3313.
[19] J.R. Lopes, W. Loh, Investigation of self-assembly and micelle polarity for a wide range of ethylene oxide–propylene oxide–ethylene oxide block copolymers in water, Langmuir 14 (1998) 750–756.
[20] E.V. Batrakova, H.Y. Han, V. Alakhov, D.W. Miller, A.V. Kabanov, Effects of Pluronic block copolymers on drug absorption in Caco-2 cell monolayers, Pharm. Res. 15 (1998) 850–855.